

See discussions, stats, and author profiles for this publication at: <https://www.researchgate.net/publication/228942247>

# DFT Study of Hydrogen Storage by Spillover on Graphene with Boron Substitution

ARTICLE *in* THE JOURNAL OF PHYSICAL CHEMISTRY C · MAY 2011

Impact Factor: 4.77 · DOI: 10.1021/jp200038b

---

CITATIONS

36

READS

181

## 4 AUTHORS, INCLUDING:



Hong-Yu Wu

Nanyang Technological University

9 PUBLICATIONS 88 CITATIONS

[SEE PROFILE](#)



Xiaofeng F Fan

Jilin University

67 PUBLICATIONS 1,183 CITATIONS

[SEE PROFILE](#)

# DFT Study of Hydrogen Storage by Spillover on Graphene with Boron Substitution

Hong-Yu Wu,<sup>†,‡</sup> Xiaofeng Fan,<sup>‡</sup> Jer-Lai Kuo,<sup>\*,§</sup> and Wei-Qiao Deng<sup>\*,†</sup>

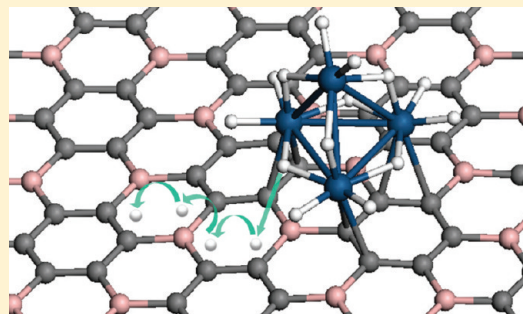
<sup>†</sup>Dalian Institute of Chemical Physics, Chinese Academy of Sciences, Dalian 116023, P. R. China

<sup>‡</sup>Division of Physics and Applied Physics, School of Physical and Mathematical Sciences, Nanyang Technological University, Singapore 637371

<sup>§</sup>Institute of Atomic and Molecular Sciences, Academia Sinica, Taipei 106, Taiwan

 Supporting Information

**ABSTRACT:** The hydrogen spillover mechanism on B-doped graphene was explicitly investigated by first-principles calculations. By the incorporation of boron into graphene, our theoretical investigation shows that B doping can substantially enhance the adsorption strength for both H atoms and the metal cluster on the substrate. The firmly bound catalytic metal on B-doped graphene can effectively dissociate H<sub>2</sub> molecules into H atoms, and the H atom is more likely to migrate from the bridge site of the H-saturated metal to the supporting graphene sheet. Further investigation on the BC<sub>3</sub> sheet gives sufficiently low activation barriers for both H migration and diffusion processes; thus, more H atoms are expected to adsorb on BC<sub>3</sub> substrate via H spillover under ambient conditions compared with the undoped graphene case. Our result is in good agreement with recent experimental findings that microporous carbon has an enhanced hydrogen uptake via boron substitution, implying that B doping with spillover is an effective approach in the modification of graphitic surface for hydrogen storage applications.



## INTRODUCTION

The lack of effective hydrogen storage medium has hindered the potential use of hydrogen as fuel for vehicles, personal electronics, and other portable power applications.<sup>1–3</sup> Some critical challenges for the storage materials involve high hydrogen storage capacity, ambient temperature operation (0–100 °C), reversibility of storage, and fast charge/release kinetics. Various candidates have been investigated, such as carbon materials,<sup>4,5</sup> metal–organic frameworks,<sup>6,7</sup> metal hydrides,<sup>8,9</sup> and microporous polymers.<sup>10,11</sup> However, no particular material can meet all the requirements thus far.

As an effective approach for hydrogen storage at ambient temperature, hydrogen spillover has been experimentally demonstrated by Yang and co-workers on many carbon-based materials, including graphite nanofibers,<sup>12</sup> carbon nanotubes,<sup>12–14</sup> activated carbons,<sup>12,14</sup> metal–organic frameworks,<sup>15–17</sup> and covalent-organic frameworks.<sup>17</sup> In these experiments, carbon substrate materials were doped with metal catalysts, which dissociated the H<sub>2</sub> molecules into H atoms. Then the H atoms migrated from metal to the supporting carbon materials and further diffused on the carbon substrate. With this hydrogen spillover process, significant enhancements of hydrogen uptake at 298 K by a factor of ca. 3 were observed, and the storage was found to be reversible with fast rates.

However, to fulfill the requirements for hydrogen storage materials, further improvement of hydrogen storage properties of

carbon materials is still needed, where a deep understanding of the hydrogen spillover process is of great importance. In this aspect, theoretical calculation can play a leading role and provide helpful information. Cheng et al. have studied the dissociation of molecular hydrogen on the Pt<sub>6</sub> cluster, and by approaching the fully saturated Pt<sub>6</sub> cluster toward the graphene sheet, they proposed a migration of two H atoms from metal to graphene, with an average activation barrier of 0.48 eV per H atom; however, thermodynamically, the migration process is endothermic.<sup>18</sup> Further investigation by Froudakis et al. about hydrogen spillover on Pt-doped graphite, which is the real case in experiments in which metal clusters are supported on the substrate, showed a rather higher migration barrier of 2.6 eV for H atom diffusing from a fully saturated Pt<sub>4</sub> cluster to the supporting graphitic surface.<sup>19</sup> Yakobson et al. also pointed out that it is difficult for a pristine graphene to attract the H atom down from the saturated metal catalyst, due to the weak C–H binding strength for the pristine graphene, which greatly inhibits the spillover process at ambient temperature.<sup>20</sup> So, how to improve the C–H binding or the hydrogen adsorption strength on the graphitic surface naturally becomes one of the crucial points in hydrogen spillover research.

**Received:** January 3, 2011

**Revised:** March 30, 2011

**Published:** April 21, 2011

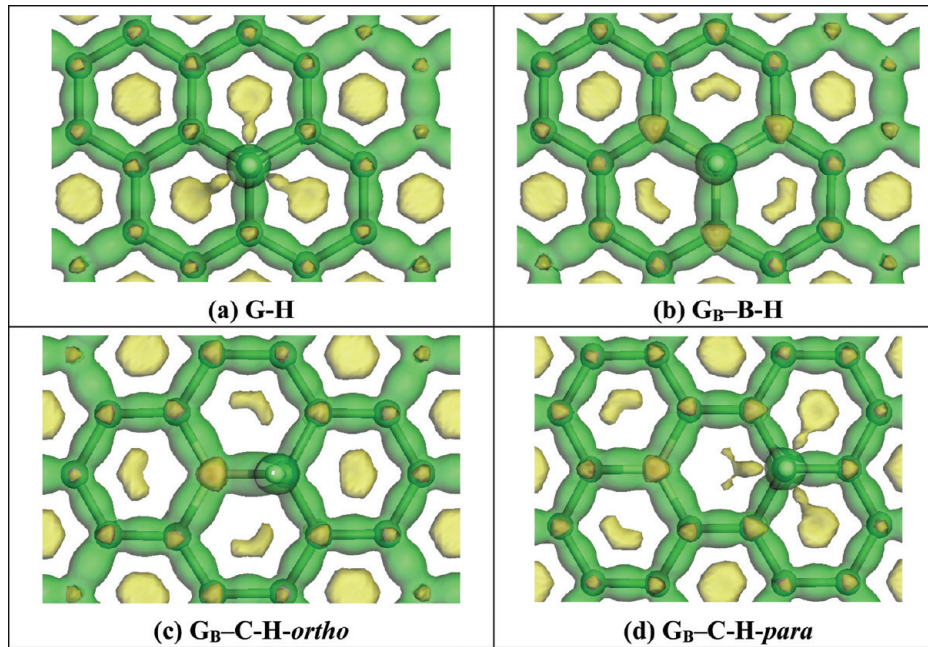


**Figure 1.** Deformation electron density isosurfaces of the four hydrogenated structures in Table 1 illustrated by top views (green, electron accumulation; yellow, electron depletion).

Recently, enhanced hydrogen adsorption was reported on boron-substituted carbon.<sup>21,22</sup> Experimental synthesis of B-doped carbon materials and their applications for hydrogen storage were also carried out.<sup>23,24</sup> Yang's group studied hydrogen storage via spillover on Ru-supported B-doped microporous carbon, and 2.2-fold enhanced hydrogen uptake of 1.2 wt % at 298 K and 10 MPa was obtained.<sup>25</sup> All the information gives a strong indication that B-doping could be an effective approach in the modification of carbon materials for hydrogen storage applications. Despite the experimental observation of enhanced hydrogen storage capacity of B-doped carbon materials with spillover method, the whole picture about the spillover mechanism, such as how the metal catalyst interacts with the B-doped carbon substrate and dissociates H<sub>2</sub> molecules, how the migration process for H atoms from metal to substrate takes place, and what the diffusion behavior of H atoms looks like in the vicinity of the hydrogenated metal on the substrate, is not yet well-understood.

In the present work, we have conducted DFT calculations to investigate the hydrogen spillover process on B-doped graphene in detail, which should be a potential candidate for hydrogen storage materials. In the simulation, we choose the Pt<sub>4</sub> cluster with tetrahedral geometry as a model to represent metal catalyst, which can effectively dissociate H<sub>2</sub> molecules and efficiently describe such kind of interactions.<sup>19</sup> We first dope only one B atom in the graphene sheet and find that the Pt<sub>4</sub> cluster is more strongly bound to the B-doped graphene compared with the undoped case. Then by putting H<sub>2</sub> molecules around the supported Pt<sub>4</sub> cluster, geometry optimization yields a saturated Pt<sub>4</sub> cluster with 14 H atoms, while Pt<sub>4</sub> supported by pure graphene can only adsorb 10 H atoms without detaching from the substrate. Second, we estimate the activation barrier for one H atom migrating from Pt<sub>4</sub> to B-doped graphene, and a much lowered migration barrier is obtained due to the enhanced C–H binding strength around the B atom. Finally, we investigate the hydrogen spillover on the BC<sub>3</sub>

sheet with a similar procedure as described above. The uniform B–C network presents sufficiently low activation barriers for both migration and diffusion of H atoms on the BC<sub>3</sub> substrate. The thermodynamic issues of hydrogen spillover on B-doped graphene are also addressed in the end.

## ■ COMPUTATIONAL METHODS

All calculations have been carried out using the DMol<sup>3</sup> program<sup>26,27</sup> based on DFT with GGA-PBE<sup>28</sup> for exchange and correlation potential. We used DFT semicore pseudopotential with double numerical basis set plus polarization functions (DNP), which is comparable with the Gaussian 6-31G(d,p) basis set in size and quality. A (6 × 6) supercell with periodic boundary conditions on the *x*–*y* plane was employed to model the infinite graphene sheet. The vacuum space was set with 20 Å in the *z* direction to avoid the interactions between periodic images. For BC<sub>3</sub> substrate, since its primitive cell is about twice the size of graphene's, a (3 × 3) supercell was used for the modeling. A 3 × 3 × 1 mesh of *k*-points<sup>29</sup> and the global orbital cutoff of 5.0 Å have been used in the spin-unrestricted calculations. All structures were relaxed without any symmetry constraints. Convergence in energy, force, and displacement was set as 10<sup>−5</sup> Ha, 0.001 Ha/Å, and 0.005 Å, respectively. All transition states were located via complete LST/QST method<sup>30</sup> as implemented in DMol<sup>3</sup> package and verified by vibrational frequency analysis. The in-plane lattice parameter of the graphene sheet has been optimized to be 2.469 Å, which is close to the ideal value of 2.46 Å. For the BC<sub>3</sub> substrate, the optimized in-plane lattice parameter is 5.178 Å, in good agreement with the value of 5.168 Å calculated by Ferro et al.<sup>21</sup>

## ■ RESULTS AND DISCUSSION

### A. Adsorption of H on Pure Graphene and 1B-Doped Graphene Sheet.

We investigated the influence of boron

**Table 1.** Calculated Hydrogen Adsorption Energy ( $\Delta E_H$ ), the Corresponding H-Bond Length ( $d_{C-H}/d_{B-H}$ ), and the Hirshfeld Charges of B and H-Bond Related Atoms, for the Hydrogenation on Pure Graphene (G) and 1B-Doped Graphene Sheet ( $G_B$ )<sup>a</sup>

G-H/ $G_B$ -H	$\Delta E_H$ (eV)	$d_{C-H}/d_{B-H}$ (Å)	Hirshfeld charge		
			B	C	H
G-H	-1.009 (1.263)	1.124	-0.019	0.060	
$G_B$ -B-H	-1.600 (0.672)	1.259	-0.063		0.020
$G_B$ -C-H-ortho	-1.933 (0.339)	1.132	0.066	-0.075	0.089
$G_B$ -C-H-para	-1.646 (0.626)	1.121	0.046	-0.011	0.075

<sup>a</sup>The value of  $\Delta E_H$  that is calculated with reference to  $1/2E_{H_2}$  is also listed in parentheses. The three lowest-energy structures for hydrogenated  $G_B$  sheet, as well as the optimized structure for hydrogenated graphene, are illustrated by side views. For clarity, only the hydrogenation regions are drawn as schematic diagrams (H, white; B, pink; C, gray).

doping on the hydrogenation of graphene sheet. Table 1 shows the calculated adsorption energy of a single H atom on pure graphene (G) and on different sites of one B atom doped graphene sheet ( $G_B$ ), the corresponding H-bond length, and the Hirshfeld charges<sup>31</sup> of relevant atoms. The schematic diagram of each stable structure we obtained after optimization is shown. For clarity, only the substrate regions involving hydrogen or Pt<sub>4</sub> cluster are drawn in the schematic diagrams in this paper, unless stated otherwise. The isosurface of deformation electron density for each structure in Table 1 is illustrated in Figure 1 to assist our analysis. Moreover, the charge states of all atoms in each structure are depicted in Figure S1 (Supporting Information), as complementary information to the density isosurface analysis. The adsorption energy of H atom ( $\Delta E_H$ ) on G/ $G_B$  sheet is calculated as

$$\Delta E_H = E_{\text{Sub}-\text{H}} - E_{\text{Sub}} - E_H \quad (1)$$

where  $E_{\text{sub}}$ ,  $E_H$ , and  $E_{\text{sub}-\text{H}}$  represent the energies of the substrate (G or  $G_B$  sheet), a single H atom, and the hydrogenated substrate, respectively. Optionally,  $\Delta E_H$  can also be calculated with reference to the half-energy of a  $H_2$  molecule  $1/2 E_{H_2}$ , instead of  $E_H$  in eq 1. Thus, both values of  $\Delta E_H$  with different reference energy are listed in Table 1 for comparison. The adsorption energy for H atom directly adsorbed on B atom in  $G_B$  sheet ( $G_B$ -B-H) is -1.600 eV, which is almost 60% enhanced hydrogenation strength with respect to that of -1.009 eV for hydrogenated graphene (G-H). In addition, we also find that when the H atom is adsorbed on the C atom next to ( $G_B$ -C-H-ortho) or opposite to ( $G_B$ -C-H-para) the B atom in the same hexagonal ring, the adsorption strength is even stronger, with  $\Delta E_H = -1.933$  eV and  $\Delta E_H = -1.646$  eV, respectively. This is in good agreement with Yang et al.'s

experimental results that doped carbon is favorable for H adsorption.<sup>25</sup>

When using  $1/2E_{H_2}$  as the reference energy, all the calculated values of  $\Delta E_H$  are positive, 2.272 eV bigger than their counterparts, as shown in the parentheses of Table 1. On one hand, the positive hydrogenation energy indicates that it is hard for the supporting G/ $G_B$  sheet to dissociate the  $H_2$  molecule directly. This is the reason why the metal catalyst is used in the hydrogen spillover process, which will be addressed in detail in the following. On the other hand, the energy difference between  $\Delta E_H$  of each structure in Table 1 is independent of the choice of energy reference. Since the hydrogen spillover process is related to the H atom diffusion behavior on the supporting substrate, we think it is more evident and convenient in formulating the H spillover mechanism by taking  $E_H$  as the reference energy. In ref 19, Froudakis et al. also used  $E_H$  as the reference energy in their H spillover study.

From the isosurface of deformation electron density, which is calculated by subtracting the electron density of the isolated atoms from the total electron density, it can be found that the electrons accumulate (green regions) between in-plane atoms to form covalent bonds on the substrate (Figure 1). Upon the hydrogenation, the in-plane  $\pi$ -electrons move upward to form a C-H bond, which results in a small depletion of electron (yellow regions) around the hydrogenated C atom (Figure 1a). Interestingly, the three depletion areas surrounding the B atom, as shown in Figure 1b, are even smaller and there is a relatively big accumulation area of electron around B. This can be attributed to boron having one less valence electron than carbon, and the doped B acts as an electron-acceptor, trapping electrons from the nearby regions. This also results in a Hirshfeld charge of -0.063 for the B atom, indicating a strong B-H bond is formed ( $G_B$ -B-H). In addition, the C atom adjacent to B is also affected by the electron clouds around B, which leads to an enhanced C-H bonding, with a Hirshfeld charge of -0.075 for the hydrogenated C ( $G_B$ -C-H-ortho). Actually, the H atom in  $G_B$ -C-H-ortho structure is not vertically bound on the top of C but leans toward the B atom, resulting in an elongated C-H bond length of 1.132 Å. Therefore, the hydrogen adsorption is considered to be cooperatively strengthened by boron and carbon. Hence, it is possible that hydrogenation is more thermodynamically favored due to the enhanced interaction between the electron of H and the  $\pi$ -cloud of the  $G_B$  sheet. To summarize, our DFT calculations suggest that B doping can greatly enhance the surface hydrogenation strength of graphene, and the C atom adjacent to B is the most favorable site for hydrogen adsorption.

**B. H<sub>2</sub> Dissociation on Pt<sub>4</sub> Cluster Supported by G or  $G_B$  Sheet.** We choose tetrahedral Pt<sub>4</sub> cluster as the representative catalyst to study the H<sub>2</sub> dissociative chemisorption on metal cluster. Since the chemisorption and desorption properties of H at full coverage are almost independent of cluster size,<sup>32</sup> a small Pt<sub>4</sub> cluster can provide us with a relatively large supercell to simulate the H diffusion process on the substrate, without losing accuracy and efficiency. To find the most stable structure for Pt<sub>4</sub> adsorbed on the supporting substrate, we tried different initial configurations by putting Pt<sub>4</sub> above C (B) site, C-C (C-B) bond, or hollow site of the hexagonal ring. As shown in Figure 2a, the Pt<sub>4</sub> cluster is attached to the graphene sheet (G-Pt<sub>4</sub>) with two Pt atoms above the C-C bonds after the optimization. The adsorption energy of Pt<sub>4</sub> on graphene  $\Delta E_{\text{Pt}}$  is calculated to be -1.184 eV. Similarly, Pt atoms also interact with the C-C and C-B bonds to form a stable structure on  $G_B$  sheet (Figure 2b,

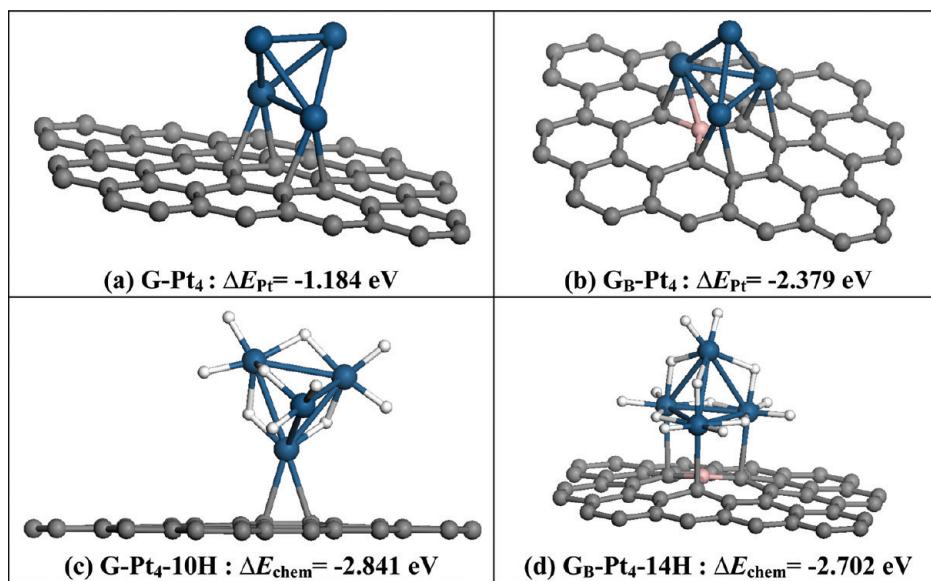


**Figure 2.** Optimized structures of (a)  $\text{Pt}_4$  cluster on pure graphene ( $\text{G}-\text{Pt}_4$ ), (b)  $\text{Pt}_4$  cluster on  $\text{G}_\text{B}$  sheet ( $\text{G}_\text{B}-\text{Pt}_4$ ), (c) saturated  $\text{Pt}_4$  cluster on graphene with 10 H atoms chemisorbed ( $\text{G}-\text{Pt}_4-10\text{H}$ ), and (d) saturated  $\text{Pt}_4$  cluster on  $\text{G}_\text{B}$  sheet with 14 H atoms chemisorbed ( $\text{G}_\text{B}-\text{Pt}_4-14\text{H}$ ). The binding strength of  $\text{Pt}_4$   $|\Delta E_{\text{Pt}}|$  on  $\text{G}_\text{B}$  sheet is 2.379 eV, much stronger than that of 1.184 eV on graphene. The chemisorption energy per H atom  $\Delta E_{\text{chem}}$  for the saturated  $\text{Pt}_4$  cluster on  $\text{G}$  and  $\text{G}_\text{B}$  sheet is  $-2.841$  and  $-2.702$  eV, respectively, indicating a strong  $\text{H}_2$  dissociation ability for the metal cluster.

$\text{G}_\text{B}-\text{Pt}_4$ ), where three Pt atoms are attached on the substrate. The corresponding adsorption strength  $|\Delta E_{\text{Pt}}|$  for  $\text{Pt}_4$  on  $\text{G}_\text{B}$  is about 2.379 eV, much stronger than that for  $\text{G}-\text{Pt}_4$ . Combining with what we have learned from the hydrogenation reaction on the  $\text{G}/\text{G}_\text{B}$  sheet, we can conclude that B-doping not only improves the hydrogen adsorption ability, but also enhances the metal binding strength for graphene sheet.

To simulate the  $\text{H}_2$  dissociation process and model the H saturation on  $\text{Pt}_4$  cluster, we initially put eight  $\text{H}_2$  molecules around the metal cluster at various locations for  $\text{G}-\text{Pt}_4$  or  $\text{G}_\text{B}-\text{Pt}_4$ . While sequential  $\text{H}_2$  adsorption behavior on the metal cluster may be of interest to some researchers in the field, it is not within the scope of this work. Without losing the contact between  $\text{Pt}_4$  and the supporting substrate after the optimization, there are totally 10 and 14 H atoms fully chemisorbed on  $\text{Pt}_4$  for  $\text{G}$  ( $\text{G}-\text{Pt}_4-10\text{H}$ ) and  $\text{G}_\text{B}$  sheet ( $\text{G}_\text{B}-\text{Pt}_4-14\text{H}$ ), respectively.<sup>33</sup>  $\text{H}_2$  molecules spontaneously dissociate onto the  $\text{Pt}_4$  cluster; i.e., a barrierless  $\text{H}_2$  dissociation process takes place, which was also reported in ref 19. As shown in Figure 2c, the  $\text{Pt}_4$  cluster is saturated with 10 H atoms, with only one Pt above the C–C bond of graphene. The average chemisorption energy per H atom  $\Delta E_{\text{chem}}$  on  $\text{Pt}_4$  is calculated by

$$\Delta E_{\text{chem}} = \frac{1}{n}(E_{\text{HnPt@Sub}} - E_{\text{Pt@Sub}} - nE_{\text{H}}) \quad (2)$$

where  $E_{\text{Pt@Sub}}$ ,  $E_{\text{HnPt@Sub}}$ , and  $n$  represent the energies of  $\text{Pt}_4$  cluster with the substrate, H-saturated  $\text{Pt}_4$  cluster with the substrate, and the number of H atoms chemisorbed on  $\text{Pt}_4$ , respectively. The  $\Delta E_{\text{chem}}$  is estimated to be  $-2.841$  eV for undoped graphene, with respect to the energy of a single H atom. It is evident that the  $\text{Pt}_4$  cluster has a tendency to detach and leaves only one Pt atom in direct contact with the graphene surface upon hydrogenation, which also indicates a weak interaction between  $\text{Pt}_4$  and graphene sheet. In contrast,  $\text{Pt}_4$  cluster on  $\text{G}_\text{B}$  sheet can fully chemisorb 14 H atoms with  $\Delta E_{\text{chem}} = -2.702$  eV, where the three Pt atoms still bind to the

underlying substrate (Figure 2d). Obviously, more hydrogen can be dissociated via the metal cluster on B-doped graphene than that in the pure graphene case. In addition, B-doping can also stabilize the  $\text{Pt}_4$  cluster upon hydrogenation, where saturated  $\text{Pt}_4$  serves as a stable H source for the subsequent hydrogen migration process.

### C. H Migration from $\text{Pt}_4$ Cluster onto the Supporting $\text{G}/\text{G}_\text{B}$ Sheet.

A key step for the hydrogen spillover to take place is how the H atoms migrate onto the supporting substrate from the metal cluster and whether the migration barrier is low enough to gain fast kinetics at room temperature. As shown in Figure 3, by dragging one H atom from the starting reactant (R) to the top of a C atom in the substrate, we carried out geometry optimization subsequently to get the final product (P). Then the transition state (TS) was searched by using complete LST/QST method,<sup>30</sup> followed by vibrational frequency calculation for further confirmation. For clarity, the red arrow is used to depict the H migration direction, pointing to the closest and unoccupied C atom on the substrate.

For the undoped graphene, in which the H atom is manually put on a C atom of graphene, we found that the H atom migrates back to the  $\text{Pt}_4$  cluster after the optimization, which means that it only forms a metastable state for the hydrogenation due to the presence of  $\text{Pt}_4$  cluster [see P(G) in Figure 3]. In this case, we thus used the constrained geometry optimization to estimate the H migration barrier, by gradually changing the Pt–H bond distance. The calculated activation barrier  $E_a(\text{G})$  for H migrating to graphene is about 2.721 eV, which is close to the reported value of 2.6 eV calculated by a different DFT functional and software package.<sup>19</sup> This comparison also validates the accuracy and reliability of our computational methods. The corresponding transition state TS(G), as illustrated in Figure 3, has the H atom away from saturated  $\text{Pt}_4$  with a Pt–H distance about 2.7 Å. There is also no C–H bond formed in TS(G), indicating an unrealistic migration process for undoped graphene. The migration reaction is actually an endothermic

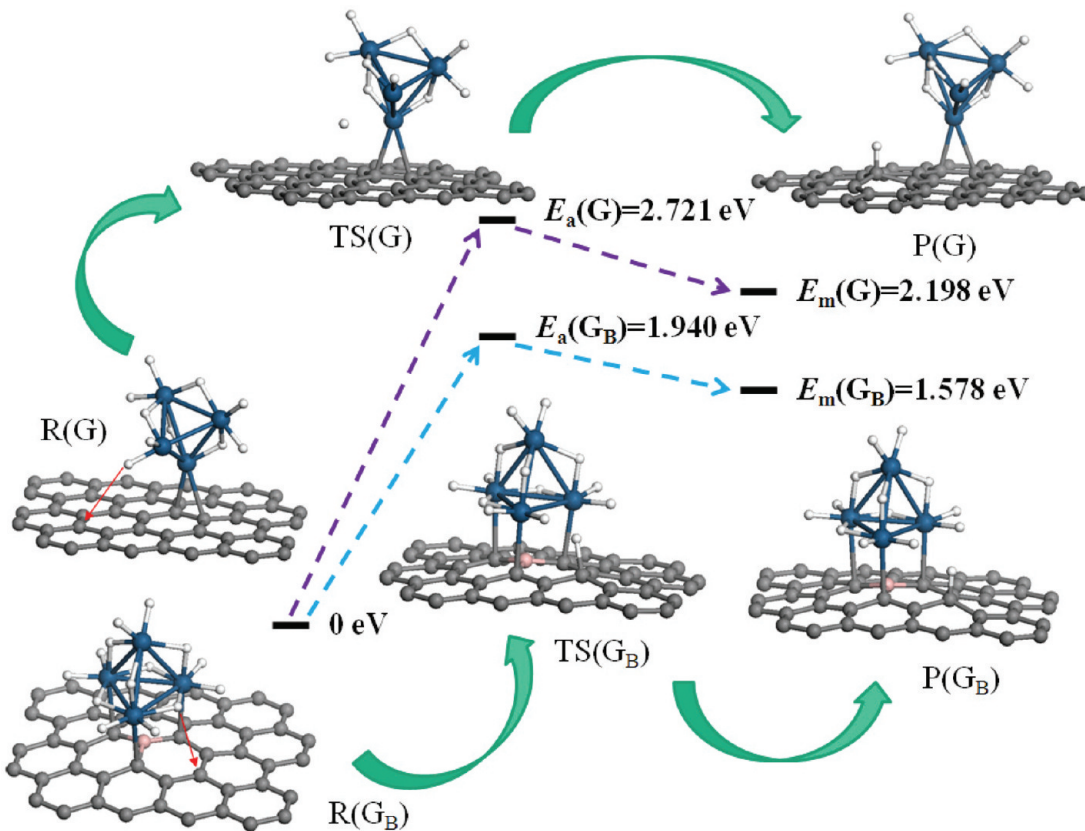


**Figure 3.** Optimized structures of initial (R), transition (TS), and final (P) states for the H migration process from saturated  $\text{Pt}_4$  cluster to the supporting G/ $\text{G}_{\text{B}}$  substrate. The black bars denote the relative energy levels of these structures, with the corresponding schematic diagrams (H, white; B, pink; C, gray; Pt, blue) drawn above or below. The calculated activation energy  $E_a$  for the H migration from  $\text{Pt}_4$  to G and  $\text{G}_{\text{B}}$  sheet is 2.721 and 1.940 eV, respectively. The purple and blue dashed arrows are respectively used to guide the eyes for the two separate migration reactions on G and  $\text{G}_{\text{B}}$  substrates. The reaction energy of the migration  $E_m$  with respect to the initial state is estimated to be 2.198 and 1.578 eV, respectively, for the G and  $\text{G}_{\text{B}}$  cases.

process, and the reaction energy  $E_m(\text{G})$  is around 2.198 eV with respect to the energy of initial state  $\text{R}(\text{G})$ . Both the high values of  $E_a(\text{G})$  and  $E_m(\text{G})$  prohibit the H migration at ambient conditions for graphene.

For the saturated  $\text{Pt}_4$  cluster on  $\text{G}_{\text{B}}$  sheet [see  $\text{R}(\text{G}_{\text{B}})$  in Figure 3], the H atom is either adsorbed on Pt (corner site) or on a Pt–Pt bond (bridge site). When we dragged one H atom from the corner site onto the C atom in the substrate, the H atom would rebind to the corner site of  $\text{Pt}_4$  cluster after optimization. Only H from the bridge site could form a stable state, binding on top of the C opposite to B in the hexagonal ring, with a C–H bond length of 1.134 Å [see  $\text{P}(\text{G}_{\text{B}})$  in Figure 3]. On one hand, H atoms are weakly bound to the bridge sites compared with those bound on the corner sites.<sup>32</sup> Therefore, the H migration from the bridge site is more likely to take place. On the other hand, from our discussions about H adsorption on  $\text{G}_{\text{B}}$  sheet, the C atom opposite to B becomes a favorable site to adsorb H with  $\Delta E_{\text{H}} = -1.646 \text{ eV}$  (see Table 1), since all the three C atoms adjacent to B are occupied by Pt atoms for  $\text{R}(\text{G}_{\text{B}})$ . The transition state  $\text{TS}(\text{G}_{\text{B}})$ , as shown in Figure 3, has an activation energy  $E_a(\text{G}_{\text{B}}) = 1.940 \text{ eV}$  for the H migration, with a C–H bond distance of 1.391 Å. The calculated imaginary frequency of  $\text{TS}(\text{G}_{\text{B}})$  is about  $-1301.1 \text{ cm}^{-1}$ . The corresponding reaction energy  $E_m(\text{G}_{\text{B}})$  is about 1.578 eV with respect to the energy of  $\text{R}(\text{G}_{\text{B}})$ . Both the activation and reaction energies have been lowered by almost 30% for the H

migration on  $\text{G}_{\text{B}}$  sheet compared with the undoped graphene case. B-doping not only enhances the H adsorption strength  $|\Delta E_{\text{H}}|$  of the substrate but also leads to averagely weakened H chemisorption strength  $|\Delta E_{\text{chem}}|$  on saturated  $\text{Pt}_4$  cluster. This eventually results in an improved thermodynamical migration reaction, accompanied by a substantially lowered activation barrier. However, the H migration is still the rate-limiting step, with an activation energy of around 2 eV for  $\text{G}_{\text{B}}$  sheet; hence, further modification on the graphene is desired to facilitate the hydrogen spillover at ambient conditions.

**D. Hydrogen Spillover on  $\text{BC}_3$  Sheet.** Capacity for H in graphitic materials has been experimentally observed to increase with boron concentration.<sup>34</sup> Kouvettakis et al. have synthesized the graphite-like  $\text{BC}_3$  compound containing 25% of boron.<sup>35</sup> Theoretical studies have suggested that bulk  $\text{BC}_3$  could be a potential candidate for hydrogen storage material.<sup>36,37</sup> The adsorption and recombination mechanism of hydrogen on the  $\text{BC}_3$  sheet has also been investigated, where both better H retention capability and easier recombination into  $\text{H}_2$  were reported.<sup>21</sup> Evidently, by increasing the boron doping content in graphene, further improvement on hydrogen spillover and more hydrogen uptake on the substrate are expected. Therefore, as a high B content model of B-doped graphene,  $\text{BC}_3$  sheet is a good substrate for studying the H spillover effect, which would be helpful in further understanding the H spillover mechanism on B-doped graphene.

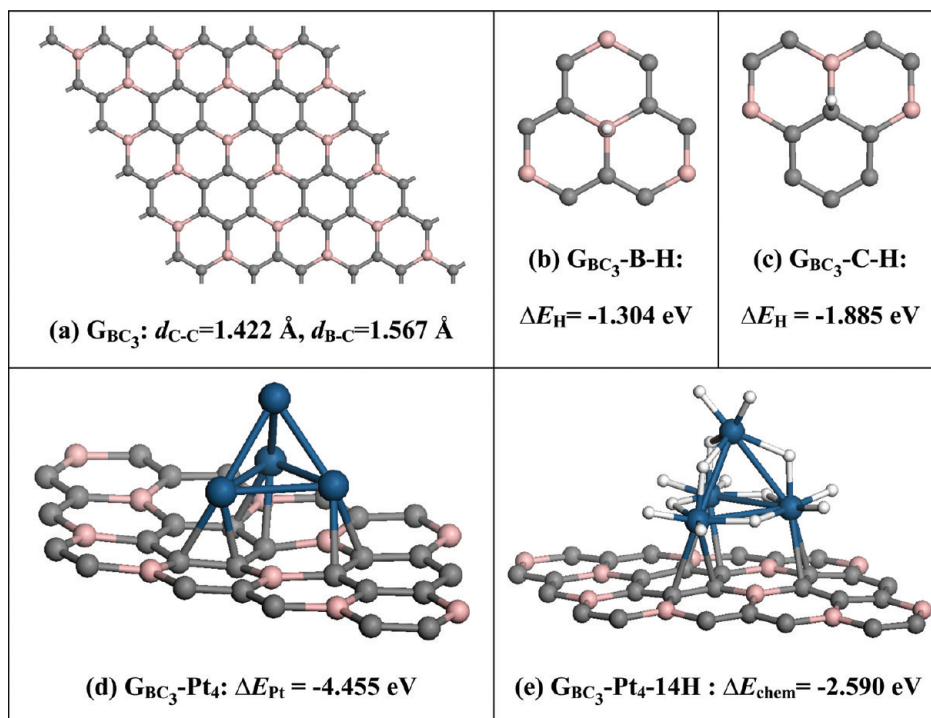


**Figure 4.** Optimized structures of (a)  $BC_3$  sheet ( $G_{BC_3}$ ), (b) H adsorption on B in  $G_{BC_3}$  ( $G_{BC_3}\text{-B-H}$ ), (c) H adsorption on C in  $G_{BC_3}$  ( $G_{BC_3}\text{-C-H}$ ), (d)  $Pt_4$  cluster on  $G_{BC_3}$  ( $G_{BC_3}\text{-Pt}_4$ ), and (e) saturated  $Pt_4$  cluster on  $G_{BC_3}$  with 14 H atoms chemisorbed ( $G_{BC_3}\text{-Pt}_4\text{-14H}$ ) (H, white; B, pink; C, gray). A  $(3 \times 3)$  supercell was used for modeling the  $BC_3$  substrate. The optimized bond length of C–C ( $d_{C-C}$ ) and B–C ( $d_{B-C}$ ) for  $G_{BC_3}$  is  $1.422 \text{ \AA}$  and  $1.567 \text{ \AA}$ , respectively.

We used a  $(3 \times 3)$  supercell for modeling the  $BC_3$  sheet ( $G_{BC_3}$ ), which is a high-symmetry substrate with the optimized C–C and B–C bond length of  $1.422$  and  $1.567 \text{ \AA}$ , respectively (Figure 4a). The high symmetry configuration of  $BC_3$  substrate we used here is the most stable structure for  $BC_3$  sheet, which was also commonly used by other groups in modeling  $BC_3$  surface.<sup>21,36,37</sup> The H atom can be adsorbed on either B (Figure 4b,  $G_{BC_3}\text{-B-H}$ ) or C atom (Figure 4c,  $G_{BC_3}\text{-C-H}$ ) in  $G_{BC_3}$  to form a stable state. Similar to the  $G_B$  case, H is more favorably bound on C ( $G_{BC_3}\text{-C-H}$ ) with an adsorption energy  $\Delta E_H = -1.885 \text{ eV}$ , compared with  $\Delta E_H = -1.304 \text{ eV}$  for  $G_{BC_3}\text{-B-H}$ . A similar procedure to that used in the  $G/G_B$  case has been implemented for finding stable structures of  $Pt_4$  and H-saturated  $Pt_4$  cluster on the  $BC_3$  sheet. As shown in Figure 4d, the  $Pt_4$  cluster is firmly bound on  $G_{BC_3}$  with three C–C bonds ( $G_{BC_3}\text{-Pt}_4$ ), and the adsorption strength  $|\Delta E_{Pt}|$  is about  $4.455 \text{ eV}$ , much stronger than that for  $G_B\text{-Pt}_4$ . Same as  $G_B\text{-Pt}_4\text{-14H}$ , the catalytic metal can accommodate up to a total of seven dissociated  $H_2$  molecules. The 14 H atoms can bind to the corner or bridge sites of the cluster (Figure 4e,  $G_{BC_3}\text{-Pt}_4\text{-14H}$ ). The average chemisorption strength per H atom  $|\Delta E_{chem}|$  for  $G_{BC_3}\text{-Pt}_4\text{-14H}$  was estimated to be  $2.590 \text{ eV}$ , which is weaker than that for  $G_B\text{-Pt}_4\text{-14H}$ .

For the  $BC_3$  sheet, we investigated the H migration process from the catalytic metal to the supporting substrate, as well as the H diffusion behavior along the C–C and C–B–C paths on  $G_{BC_3}$ . The reaction diagram of each migration/diffusion process is plotted in Figure 5, together with the top views of the critical structures involved in these reactions. Figure 5a shows the schematic energy profile along the reaction coordinate for H migrating from Pt–Pt bond to C on the  $BC_3$  sheet. A sufficiently lowered activation

barrier  $E_a$  of  $0.648 \text{ eV}$  has been obtained for H migration from  $Pt_4$  to  $G_{BC_3}$ . A fast kinetics for H migration thus can be achieved under ambient conditions. However, the migration process remains thermodynamically unfavored, where the energy of final state (FS1) is about  $0.639 \text{ eV}$  with respect to that of initial state (IS), only  $9 \text{ meV}$  lower than that of transition state (TS1), whose imaginary frequency is around  $-754.0 \text{ cm}^{-1}$ . The C–H bond length is  $1.457$  and  $1.280 \text{ \AA}$  for TS1 and FS1, respectively.

Further diffusion of H atom away from the vicinity of the catalytic metal can make full use of surface sites of the substrate for hydrogen storage applications. For the  $BC_3$  sheet, two distinct diffusion paths were investigated following the H migration process. The H atom first diffuses from FS1 to FS2 along the C–C path, as shown in Figure 5b, and undergoes an activation barrier of  $0.52 \text{ eV}$ . The corresponding transition state (TS2) has an imaginary frequency of  $-742.9 \text{ cm}^{-1}$ . The diffusion reaction along the C–C path is exothermic, with the reaction energy being  $-0.047 \text{ eV}$  with respect to the energy of FS1. Then, H further diffuses from FS2 to FS3 via the C–B–C path. It turns out to be a little endothermic, and the energy of FS3 is about  $0.153 \text{ eV}$  larger than that of FS2, as seen in Figure 5c. The B atom adsorbs H and forms an intermediate state (IMS) in the middle of the C–B–C path, where two transition states (TS3, TS4) close to IMS are located, with the energy of TS3 (TS4) being around  $0.66 \text{ eV}$  higher than that of FS2. The imaginary frequencies of TS3 and TS4 are calculated to be  $-773.1$  and  $-740.8 \text{ cm}^{-1}$ , respectively. Both activation barriers are sufficiently low for H diffusion along the C–C and C–B–C paths, indicating that a fast H diffusion on the substrate can be achieved under ambient conditions.

Combining the data we obtain for  $G$ ,  $G_B$ , and  $G_{BC_3}$  cases, we find a strong dependence of H migration energy  $E_m$  on the

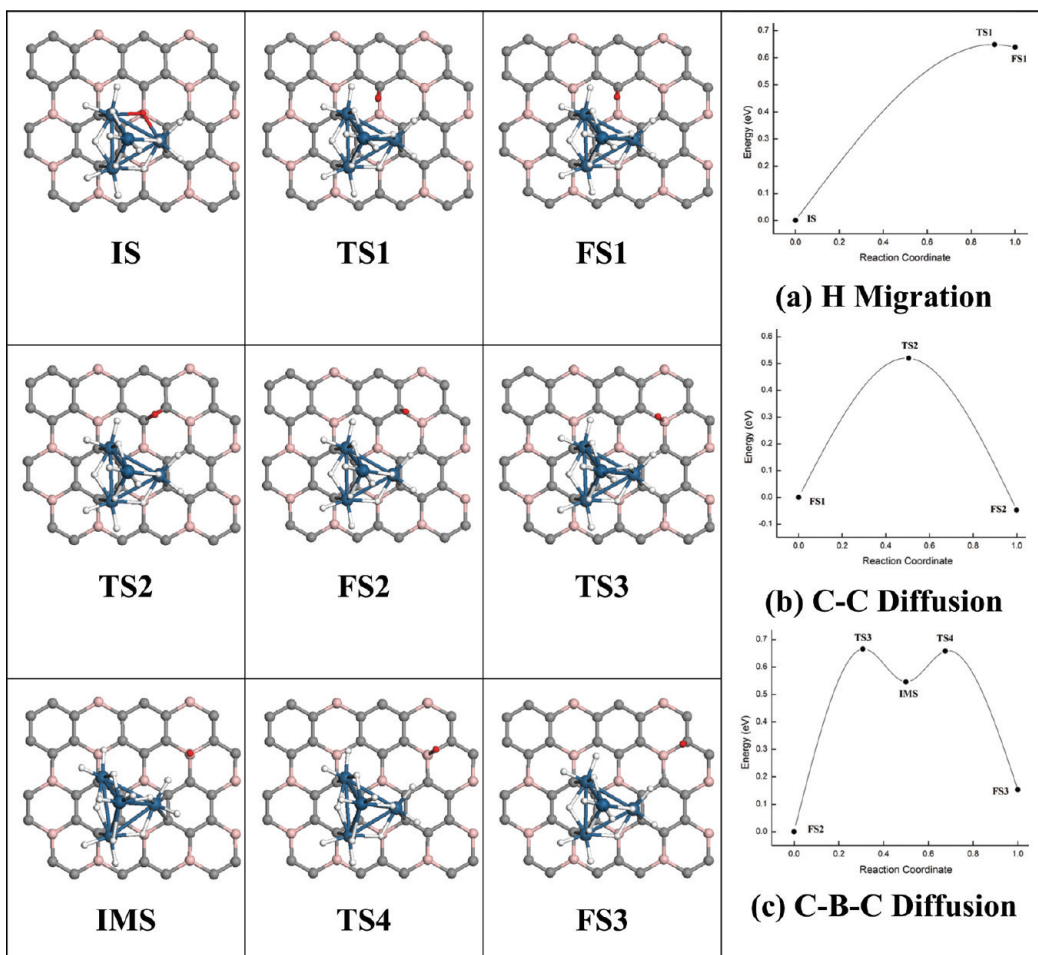


**Figure 5.** Calculated reaction diagrams of (a) H migration from saturated  $\text{Pt}_4$  to C on the  $\text{BC}_3$  sheet, (b) H diffusion along the C–C path on  $\text{G}_{\text{BC}_3}$ , and (c) H diffusion along the C–B–C path on  $\text{G}_{\text{BC}_3}$ . The schematic diagrams of initial (IS), transition (TS), intermediate (IMS), and final (FS) states involved in the reactions are illustrated by top views (H, white; B, pink; C, gray; Pt, blue). The reactive H atom is highlighted by red. The lines that link critical points are used to guide the eyes. The energy of reactant in each reaction diagram is set to be zero.

hydrogenation strength  $|\Delta E_{\text{H}}|$  of the substrate. As shown in Figure 6, from G to  $\text{G}_{\text{BC}_3}$ , the reaction energy  $E_m$  for H migration decreases as the H adsorption strength  $|\Delta E_{\text{H}}|$  of the supporting sheet increases; i.e., there is a downward trend of  $\Delta E_{\text{H}}$  toward the binding energy of  $\text{H}_2$  molecule per H atom  $E_{\text{H-bind}} = -2.272$  eV. In contrast, the average H chemisorption energy  $\Delta E_{\text{chem}}$  exhibits an upward though not obvious trend toward  $\Delta E_{\text{H-bind}}$  on the energy profile. The energy difference between  $\Delta E_{\text{H}}$  and  $\Delta E_{\text{chem}}$  is reduced to 0.705 eV for the  $\text{G}_{\text{BC}_3}$  sheet, compared with that of 1.832 eV for the undoped graphene. The decreased energy difference surely draws closer the energies of initial and final states involved in the H migration reaction, thus resulting in an improved thermodynamical H migration process. Noticeably seen from Figure 6, since  $\Delta E_{\text{H}}$  is higher than  $E_{\text{H-bind}}$  on the energy profile, it is hard for the substrate to chemisorb H atoms directly from  $\text{H}_2$  gas. The reported activation barrier for direct  $\text{H}_2$  dissociation on the  $\text{BC}_3$  sheet was about 1.2 eV,<sup>21</sup> much higher than our calculated H migration barrier of 0.648 eV from  $\text{Pt}_4$  to  $\text{G}_{\text{BC}_3}$ . Thus, the metal cluster not only plays the catalytic role in dissociating  $\text{H}_2$  molecules but also shows the great advantage of H spillover method in the hydrogen storage study by providing a sufficiently low activation barrier for H adsorption on the substrate.

Furthermore, under ambient conditions usually a small endothermic reaction is affordable. The  $\text{BC}_3$  sheet is a high-symmetry substrate, with boron atoms uniformly distributed. The C atoms in  $\text{G}_{\text{BC}_3}$  are equivalent with the same  $\Delta E_{\text{H}}$ ; thus, the H diffusion process on the  $\text{G}_{\text{BC}_3}$  sheet is thermodynamically favored or experimentally affordable under ambient conditions. As for the H migration process, the endothermic reaction can be improved by either enhancing  $|\Delta E_{\text{H}}|$  of B-doped graphene or using other metal catalyst with smaller  $|\Delta E_{\text{chem}}|$  than that of  $\text{Pt}_4$ . Since the H adsorption strength  $|\Delta E_{\text{H}}| = 1.885$  eV for  $\text{G}_{\text{BC}_3}$ –C–H is weaker than  $|\Delta E_{\text{H}}| = 1.933$  eV for  $\text{G}_\text{B}$ –C–H-ortho, a moderately B-doped graphene with boron uniformly distributed plus a proper catalytic metal may be a better candidate for hydrogen storage applications via hydrogen spillover, which would need further investigation in our future work.

## SUMMARY

In summary, by introducing B atoms into graphene, DFT calculations show substantially enhanced hydrogen adsorption strength for C atoms around B on the substrate, where the catalytic metal can also be firmly absorbed and further dissociate more  $\text{H}_2$  molecules into H atoms. Upon H-saturation on the

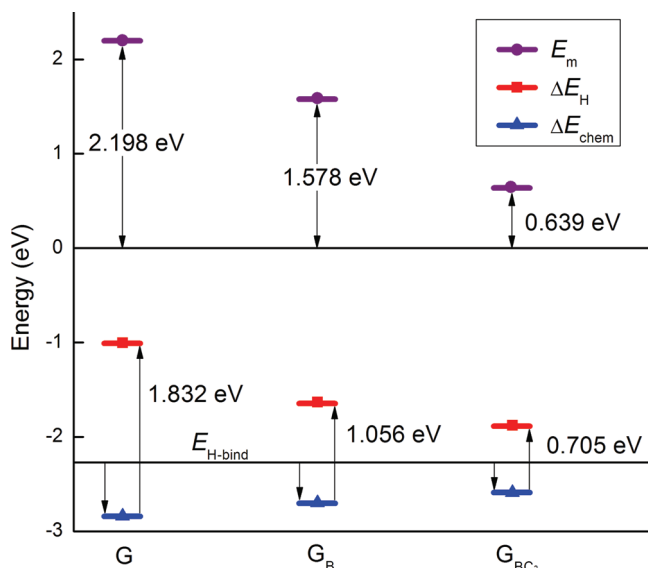


**Figure 6.** Evolution profiles of migration reaction energy  $E_m$ , hydrogen adsorption energy  $\Delta E_H$  and average H chemisorption energy  $\Delta E_{\text{chem}}$  for the G,  $G_B$ , and  $G_{BC_3}$  sheets. The binding energy of  $H_2$  molecule per H atom  $E_{H\text{-bind}} = -2.272$  eV is denoted with a horizontal line. The single-headed arrow line points downward from  $E_{H\text{-bind}}$  to  $\Delta E_{\text{chem}}$ , indicating the energetically favored  $H_2$  dissociation process on the catalytic metal, and then points upward from  $\Delta E_{\text{chem}}$  to  $\Delta E_H$ , showing that the H migration from metal to substrate is endothermic. The difference between  $\Delta E_{\text{chem}}$  and  $\Delta E_H$  is labeled beside the single-arrow line.

metal cluster, H atom is more likely to migrate from the bridge site of the cluster onto the supporting sheet. Due to reduced energetic difference between  $\Delta E_H$  and  $\Delta E_{\text{chem}}$ , an improved thermodynamical H migration process can be achieved on B-doped graphene. Both H migration and diffusion processes are investigated to have sufficiently low activation barriers, indicating that more H atoms can adsorb on B-doped graphene than on the undoped graphene under ambient conditions. By simulating the whole hydrogen spillover process, our work not only interprets the catalytic mechanism of the H spillover on B-doped graphene but also supports the experimental findings that B-doped micro-porous carbon has an enhanced hydrogen storage capacity.<sup>25</sup> Our calculations conclude that B doping with catalytic metal on the substrate is an effective method of modifying the graphitic surface for hydrogen storage applications.

## ■ ASSOCIATED CONTENT

**S Supporting Information.** The charge states of all atoms in each structure of Table 1 (Figure S1). This material is available free of charge via the Internet at <http://pubs.acs.org>.

## ■ AUTHOR INFORMATION

### Corresponding Author

\*E-mail: jlkao@pub.iams.sinica.edu.tw (J.-L.K.); dengwq@dicp.ac.cn (W.-Q.D.).

## ■ ACKNOWLEDGMENT

This work was supported by the “100-Talent Program” of the Chinese Academy of Sciences, NSFC grant no. 20833008,

Nanyang Technological University, Academia Sinica, and the National Science Council of Taiwan.

## ■ REFERENCES

- (1) Schlapbach, L.; Zuttel, A. *Nature* **2001**, *414*, 353.
- (2) Satyapal, S.; Petrovic, J.; Read, C.; Thomas, G.; Ordaz, G. *Catal. Today* **2007**, *120*, 246.
- (3) Crabtree, G. W.; Dresselhaus, M. S. *MRS Bull.* **2008**, *33*, 421.
- (4) Deng, W. Q.; Xu, X.; Goddard, W. A. *Phys. Rev. Lett.* **2004**, *92*, 166103.
- (5) Yang, Z. X.; Xia, Y. D.; Mokaya, R. *J. Am. Chem. Soc.* **2007**, *129*, 1673.
- (6) Rowsell, J. L. C.; Yaghi, O. M. *Angew. Chem.-Int. Ed.* **2005**, *44*, 4670.
- (7) Han, S. S.; Deng, W. Q.; Goddard, W. A. *Angew. Chem.-Int. Ed.* **2007**, *46*, 6289.
- (8) Chen, P.; Xiong, Z. T.; Luo, J. Z.; Lin, J. Y.; Tan, K. L. *Nature* **2002**, *420*, 302.
- (9) Ronnebro, E.; Majzoub, E. H. *J. Phys. Chem. B* **2007**, *111*, 12045.
- (10) Lee, J. Y.; Wood, C. D.; Bradshaw, D.; Rosseinsky, M. J.; Cooper, A. I. *Chem. Commun.* **2006**, 2670.
- (11) Li, A.; Lu, R. F.; Wang, Y.; Wang, X.; Han, K. L.; Deng, W. Q. *Angew. Chem.-Int. Ed.* **2010**, *49*, 3330.
- (12) Lueking, A. D.; Yang, R. T. *Appl. Catal., A* **2004**, *265*, 259.
- (13) Lueking, A.; Yang, R. T. *J. Catal.* **2002**, *206*, 165.
- (14) Lachawiec, A. J.; Qi, G. S.; Yang, R. T. *Langmuir* **2005**, *21*, 11418.
- (15) Li, Y. W.; Yang, R. T. *J. Am. Chem. Soc.* **2006**, *128*, 726.
- (16) Li, Y. W.; Yang, R. T. *J. Am. Chem. Soc.* **2006**, *128*, 8136.
- (17) Li, Y. W.; Yang, R. T. *AIChE J.* **2008**, *54*, 269.
- (18) Chen, L.; Cooper, A. C.; Pez, G. P.; Cheng, H. *J. Phys. Chem. C* **2007**, *111*, 18995.
- (19) Psوفogianakis, G. M.; Froudakis, G. E. *J. Phys. Chem. C* **2009**, *113*, 14908.
- (20) Singh, A. K.; Ribas, M. A.; Yakobson, B. I. *ACS Nano* **2009**, *3*, 1657.
- (21) Ferro, Y.; Marinelli, F.; Jelea, A.; Allouche, A. *J. Chem. Phys.* **2004**, *120*, 11882.
- (22) Zhu, Z. H.; Lu, G. Q.; Hatori, H. *J. Phys. Chem. B* **2006**, *110*, 1249.
- (23) Chung, T. C. M.; Jeong, Y.; Chen, Q.; Kleinhammes, A.; Wu, Y. *J. Am. Chem. Soc.* **2008**, *130*, 6668.
- (24) Jeong, Y.; Chung, T. C. M. *Carbon* **2010**, *48*, 2526.
- (25) Wang, L. F.; Yang, F. H.; Yang, R. T. *AIChE J.* **2009**, *55*, 1823.
- (26) Delley, B. *J. Chem. Phys.* **1990**, *92*, 508.
- (27) Delley, B. *J. Chem. Phys.* **2000**, *113*, 7756.
- (28) Perdew, J. P.; Burke, K.; Ernzerhof, M. *Phys. Rev. Lett.* **1996**, *77*, 3865.
- (29) Monkhorst, H. J.; Pack, J. D. *Phys. Rev. B* **1976**, *13*, 5188.
- (30) Govind, N.; Petersen, M.; Fitzgerald, G.; King-Smith, D.; Andzelm, J. *Comput. Mater. Sci.* **2003**, *28*, 250.
- (31) Hirshfeld, F. L. *Theor. Chim. Acta* **1977**, *44*, 129.
- (32) Zhou, C. G.; Wu, J. P.; Nie, A. H.; Forrey, R. C.; Tachibana, A.; Cheng, H. S. *J. Phys. Chem. C* **2007**, *111*, 12773.
- (33) Close contact between the  $Pt_4$  cluster and the G or  $G_B$  sheet can provide a steady H flow from the metal cluster to the supporting substrate; otherwise, the long distance between the chemisorbed H atom and the surface C atom will definitely increase the hydrogen migration barrier from metal to substrate, thus weakening the hydrogen spillover effect. For  $G_B-Pt_4$ , seven  $H_2$  molecules are fully dissociated onto the  $Pt_4$  cluster, with only one  $H_2$  departing away after optimization. However, the  $Pt_4$  cluster will detach from the undoped graphene sheet, when eight  $H_2$  molecules are initially put around the metal cluster. Therefore, we gradually decrease the number of  $H_2$  put around the  $Pt_4$  in the initial arrangement and reoptimize the structure until we get a saturated  $Pt_4$  without flying away from the substrate.

- (34) Schenk, A.; Winter, B.; Lutterloh, C.; Biener, J.; Schubert, U. A.; Kuppers, J. *J. Nucl. Mater.* **1995**, *222*, 767.
- (35) Kouvetsakis, J.; Kaner, R. B.; Sattler, M. L.; Bartlett, N. *J. Chem. Soc. Chem. Commun.* **1986**, 1758.
- (36) Zhang, C. J.; Alavi, A. *J. Chem. Phys.* **2007**, *127*, 214704.
- (37) Sha, X. W.; Cooper, A. C.; Bailey, W. H.; Cheng, H. S. *J. Phys. Chem. C* **2010**, *114*, 3260.